UNIVERSIDAD REGIONAL AMAZÓNICA IKIAM
Facultad Ciencias de la Tierra y Agua
Carrera en Geociencias

Dinámica de los incendios forestales en función de la sequía hidrológica y meteorológica en la Amazonía

Naomi Nicole Toledo Rojas

Tena, enero 2022
Napo, Ecuador

DECLARACIÓN DE DERECHO DE AUTOR, AUTENTICIDAD Y RESPONSABILIDAD

Tena, 28 de septiembre de 2021

Yo, Naomi Nicole Toledo Rojas con documento de identidad N° 1105726317, declaro que los resultados obtenidos en la investigación que presento en este documento final, previo a la obtención del título Ingeniero en Geociencias son absolutamente inéditos, originales, auténticos y personales.

En virtud de lo cual, el contenido, criterios, opiniones, resultados, análisis, interpretaciones, conclusiones, recomendaciones y todos los demás aspectos vertidos en la presente investigación son de mi autoría y de mi absoluta responsabilidad.

Por la favorable atención a la presente, suscribo de usted,

Atentamente,

Firma:

_____

Naomi Nicole Toledo Rojas

Certificado de dirección de trabajo de integración curricular

Certifico que el trabajo de integración curricular titulado: “Dinámica de los incendios forestales en función de la sequía hidrológica y meteorológica en la Amazonía”, en la modalidad de: proyecto de investigación en formato artículo original, fue realizado por: Naomi Nicole Toledo Rojas, bajo mi dirección.

El mismo ha sido revisado en su totalidad y analizado por la herramienta de verificación de similitud de contenido; por lo tanto, cumple con los requisitos teóricos, científicos, técnicos, metodológicos y legales establecidos por la Universidad Regional Amazónica Ikiam, para su entrega y defensa.

Tena, 04 de octubre de 2021

Firma:

Firmado electrónicamente por:
BRUNO PIRILO

……

Bruno Pirilo Conicelli
C.I: 1759149774

AGRADECIMIENTOS

Un profundo agradecimiento a:

PhD. Bruno Conicelli mi tutor de tesis, quien con su conocimiento y apoyo oportuno ha permitido mi crecimiento profesional.

PhD. Gabriel M. Moulatlet, quien me ha apoyado durante el proceso de corrección de la investigación.

PhD. Gabriel Gaona, por sus aportes y enseñanzas sobre Analisis Espaciales en R.

Universidad Regional Amazónica Ikiam y sus docentes, especialmente a los de la Carrera de Geociencias, quienes mediante sus enseñanzas han contribuido a mi formación profesional y personal.

DEDICATORIA

A mis padres, por su amor, dedicación y sacrificio durante el transcurso de mi vida.

A mi hermano, por su apoyo incondicional y ser mi inspiración para luchar cada día.

A mi prima, por su cariño y ser un pilar fundamental.

A mis amigos, que se convirtieron en familia al ayudarme y compartir los mejores momentos.

ÍNDICE GENERAL

ÍNDICE DE FIGURAS

RESUMEN

Durante las últimas décadas, los incendios forestales antropogénicos han ido modificando la dinámica de la vegetación en la Amazonia. Aunque prácticamente todos los incendios se inician por acción antrópica, su amplificación puede estar relacionada con las condiciones climáticas, como las sequías asociadas a la fase cálida de El Niño. Determinar el comportamiento de las sequías es, por tanto, fundamental para predecir la propagación de los incendios en la Amazonía. Las mediciones de sequía se basan generalmente en el índice de precipitación mediante observaciones remotas (datos meteorológicos) o mediciones *in situ* del nivel del agua (datos hidrológicos). Cuando una sequía meteorológica se prolonga, puede desencadenar una sequía hidrológica, por lo que es necesario conocer el estado de la sequía a diferentes profundidades del suelo. Las medidas complementarias, como el *Indicador de Sequía Hidrológica*, son útiles para comprender la intensidad de la sequía en el subsuelo. Este estudio evalúa la dinámica de los incendios en la Amazonía en función de la sequía meteorológica e hidrológica asociada a El Niño entre los años 2004-2016. Encontramos una tendencia hacia la amplificación de los incendios forestales en áreas con una alta correlación (R = 0,72, P = 0,01) entre sequía hidrológica y meteorológica. También observamos que los años 2015-2016 presentaron una intensidad de El Niño muy fuerte, con un incremento del 244% en el área quemada anual promedio en áreas con sequía extrema en comparación con áreas sin condiciones de sequía. Nuestros resultados sugieren que las posibles áreas donde los incendios tienden a aumentar están generalmente sujetas a sequías hidrológicas, amplificándose en regiones donde los efectos de El Niño son más intensos. Comprender este comportamiento puede ser útil para determinar la susceptibilidad de áreas de la selva amazónica a la ocurrencia de incendios.

Palabras Claves

Incendios Forestales, Amazonía, Indicador de Sequía (DI), Índice de Precipitación Estandarizado (SPI), El Niño-Oscilación del Sur (ENSO).

ABSTRACT

During the last decades, anthropogenic forest fires have been modifying vegetational dynamics of the Amazon Forest. Although practically all fires start by anthropic action, their amplification can be related to climatic conditions, such as the droughts associated with the warm El Niño phase. Determining the behavior of droughts is, thus, essential to predict the spread of fires in the Amazon. Drought measurements are generally based on precipitation index by on remote observations (meteorological data) or *in-situ* measurements of water level (hydrological data). When a meteorological drought is prolonged, it can trigger a hydrological drought, making it necessary to know the state of the drought at different depths in the soil. Complementary measures, such as the *Hydrological Drought Indicator*, are helpful to understand the intensity of the drought in the subsoil. This study evaluates the dynamics of fires in the Amazon as a function of the meteorological and hydrological drought associated with El Niño between the years 2004-2016. We found a trend towards amplifying forest fires in areas with a high correlation ($R = 0.72$, $P = 0.01$) between hydrological and meteorological drought. We also observed that the 2015-2016 years presented a very strong El Niño intensity, with a 244% increment in the average annual burned area in areas with extreme drought compared to areas with non-drought conditions. Our results suggest that the possible areas where fires tend to increase are generally subject to hydrological droughts, being amplified in regions where the effects of El Niño are more intense. Understanding this behavior can be helpful to determine the susceptibility of areas of the Amazon Forest to the occurrence of fires.

Keywords

Wildfires, Amazon, Drought Indicator (DI), Standardized Precipitation Index (SPI), El Niño-Southern Oscillation (ENSO).

Dynamics of wildfires as a function of hydrological and meteorological droughts in Amazonia

Abstract

During the last decades, anthropogenic forest fires have been modifying vegetational dynamics of the Amazon Forest. Although practically all fires start by anthropic action, their amplification can be related to climatic conditions, such as the droughts associated with the warm El Niño phase. Determining the behavior of droughts is, thus, essential to predict the spread of fires in the Amazon. Drought measurements are generally based on precipitation index by on remote observations (meteorological data) or *in-situ* measurements of water level (hydrological data). When a meteorological drought is prolonged, it can trigger a hydrological drought, making it necessary to know the state of the drought at different depths in the soil. Complementary measures, such as the *Hydrological Drought Indicator*, are helpful to understand the intensity of the drought in the subsoil. This study evaluates the dynamics of fires in the Amazon as a function of the meteorological and hydrological drought associated with El Niño between the years 2004-2016. We found a trend towards amplifying forest fires in areas with a high correlation ($R = 0.72$, $P = 0.01$) between hydrological and meteorological drought. We also observed that the 2015-2016 years presented a very strong El Niño intensity, with a 244% increment in the average annual burned area in areas with extreme drought compared to areas with non-drought conditions. Our results suggest that the possible areas where fires tend to increase are generally subject to hydrological droughts, being amplified in regions where the effects of El Niño are more intense. Understanding this behavior can be helpful to determine the susceptibility of areas of the Amazon Forest to the occurrence of fires.

1 Introduction

Forest fires in the Amazon cause loss of vegetation cover and represent a threat to biodiversity (Y. Chen et al., 2013). In addition, the disturbances caused by fires on the carbon and hydrological cycles influence the global climate and generate uncertainties in future climate projections (Baker et al., 2009). Most forest fires in the Amazon are associated with anthropogenic actions, such as deforestation of large areas for agriculture (Tang & Arellano, 2017). In the past decades, the years with the highest frequency and

severity of forest fires coincided with the warm phase of El Niño-Southern Oscillation (ENSO), correlated with a decrease in precipitation in the Amazon basin (Ropelewski & Halpert, 1987; Taufik et al., 2017; Yoon & Zeng, 2010). In addition, abnormal warming of sea surface temperatures (SST) in the North Atlantic causes a northward shift of the Intertropical Convergence Zone (ITCZ), reducing rainfall in the west and south of the Amazon basin (Y. Chen et al., 2013; Yoon & Zeng, 2010). For instance, there is a high correlation between the cumulative number of fires during the dry season and the increasing in SST before the fire season (Y. Chen et al., 2011). Droughts in the hydrological cycle are defined by precipitation decline that causes a deficit of soil moisture, followed by a decrease in current flows and groundwater levels (Changnon, 1987). Droughts can be classified according to their effect on the hydrological cycle (Gerdener et al., 2020). The meteorological drought is the deficiency of precipitation in a region during a certain period of time (Belal & El-ramady, 2014).The hydrological drought refers to the deficits of accessible water in the storage of water in surface and underground reservoirs concerning standard conditions (Gerdener et al., 2020). Therefore, groundwater levels in unconfined or semi-confined aquifers indicate meteorological conditions that occur on time scales from days to years. While, near-surface water storage corresponds to the amount of precipitation. Drought monitoring is generally based on *in situ* measurements of precipitation or river levels (J. L. Chen et al., 2009; Houborg et al., 2012). However, indicator of drought intensity such as groundwater storage measurements are not always incorporated in absence of direct measurements in space and time (B. F. Thomas et al., 2017). Thus, to understand drought events, measurements of meteorological and hydrological droughts are necessary. The satellite observations of the Gravity Recovery and Climate Experiment (GRACE) mission (Tapley et al., 2019), allow the detection of the terrestrial water storage (TWS), integrating soil moisture, snow water equivalent, surface water from vegetation cover and groundwater storage (Yin et al., 2020). However, the information generated by GRACE can only be separated into individual hydrological components through auxiliary data (Zheng et al., 2012). The GRACE Data Assimilation System, based on the Catchment Land Surface Model, improves the value of TWS data by allowing space-time scaling and vertical decomposition of the moisture components. Thus, it is possible to address hydrological drought by using drought indicators (DI) for surface

soil moisture (sfsm), root zone soil moisture (rtzsm) and groundwater (gws). The current humidity conditions in each of these soil zones are expressed as the probability of occurrence of drought events, with low drought indicator defines as values soil moisture drier than average, and high values indicating soil moisture wetter than average (Houborg et al., 2012). Therefore, the DI provides information on the severity of the drought in a given site and can contribute to the distinction of hydrological drought based on the subsoil depth (Nie et al., 2017). However, the DI to level sfsm is based on the moisture at the surface level, a factor that is generally included during the calculation of meteorological droughts. Therefore, it is essential to determine if there is a response time between the DI to level of sfsm and meteorological drought measurements. The characterization of the meteorological drought can be done by using the standardized precipitation index (SPI) (Y. Chen et al., 2013; McKee et al., 1993), since it can be calculated on different time scales and depends solely on precipitation, without the need for auxiliary variables. Furthermore, SPI is also related to soil moisture (Nie et al., 2017; Wang et al., 2019). The Amazon basin experienced exceptional droughts, during the years 2005 and 2010 where the Central and Southern parts of the basin were the most affected (J. L. Chen et al., 2009; Espinoza et al., 2011). In 2015 and 2016, a climatological water deficit was recorded in the region, with the highest occurrence of fires with a burned area of approximately 9246 km2 (Berenguer et al., 2021; Pontes-Lopes et al., 2021). Therefore, this study aims to (1) evaluate the temporal distribution of the hydrological drought at different levels of soil moisture; (2) analyze the relationship between the DI of surface soil moisture and the SPI. And (3) evaluate the behavior of the ENSO hydrological drought and relate it to the area affected by wildfires in the Amazon for the period between the year 2004 to 2016.

2 Data and Methods

2.1 Geographic context

The study area (Figure 1) corresponds to the Amazon river basin, with an area of approximately 7.4 million km² (Benton, 1963). The Amazon River transports around 0.75 km³/h of water to the Atlantic.

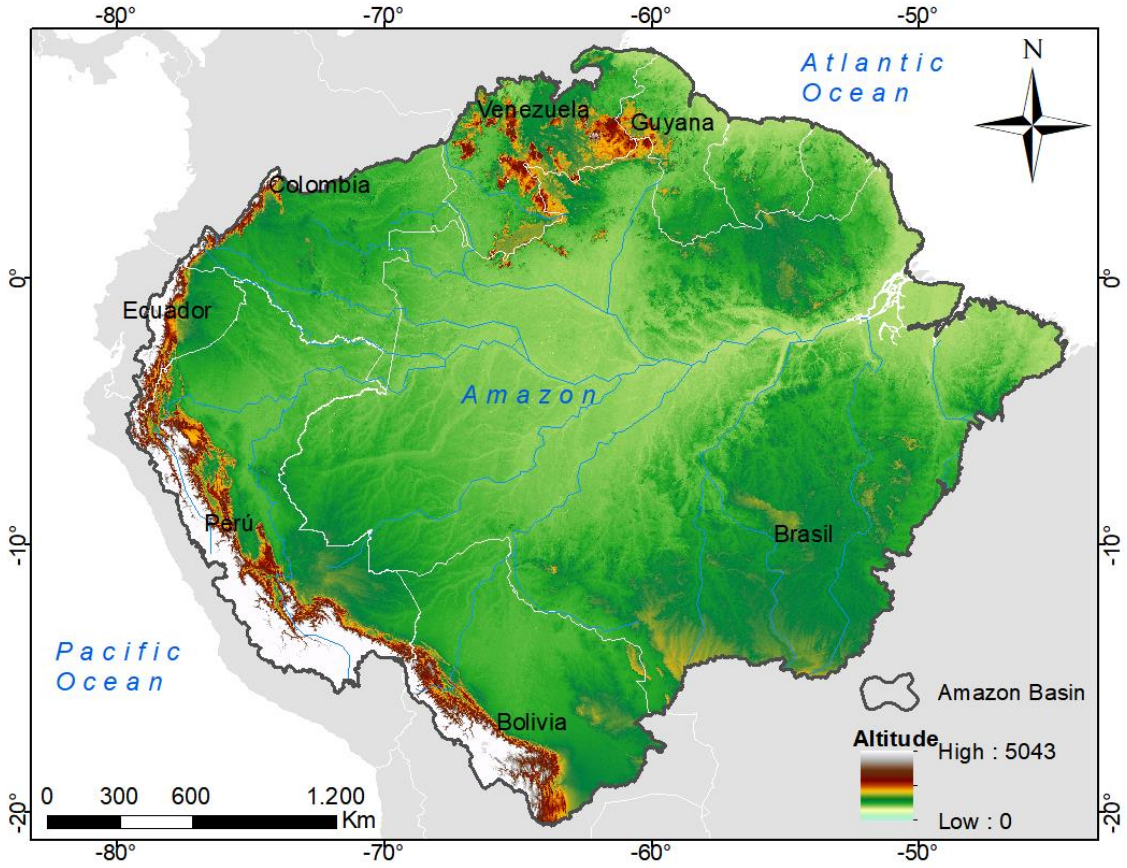

Figure 1. Location map of the Amazon basin in South America. The black line delimits the perimeter of the Amazon basin. Elevation information is shown in the background. Low elevations are depicted in green shades and high elevations in red shades.

2.2 Drought Indicators (DIs)

The DI (https://nasagrace.unl.edu/), are available on a global scale at a resolution of 0.25 degrees for each week and show the severity of the drought classified into five categories: abnormal (20-30%), moderate (10-20%), severe (5-10%), extreme (2-5%) and exceptional (0-2%) (Houborg et al., 2012). The temporal distribution of DI was evaluated for the years 2004-2019, using two metrics based on monthly values: the annual average and the annual

minimum of percentiles of soil moisture at the sfsm, rtzsm and gws levels. To evaluate the DI time series dynamics, the classical X11 decomposition method (Dagum & Bianconcini, 2010), was applied, which realize for the decomposition and seasonal adjustment of the monthly series based on an iterative principle using moving averages (Ladiray & Quenneville, 2001).

2.3 Change of DI and burned fraction area a function of time

The burned fraction area (bf) monthly data set from year 2004 to 2016 was obtained from the GFED4 database (https://globalfiredata.org/pages/data/#burned-area), which provides the monthly bf, at a spatial resolution of 0.25 degrees. The rate of change to increase or decrease the bf and DI at the level of sfsm, rtzsm and gws during the study period, were analyzed using a linear model fitted with ordinary least squares using the function 'lm.fit' (Pappo et al., 2021). For the calculation of the slope(rate of change) of the linear model was used the function 'coefficients'. To calculate the slope of the linear model, the 'coefficients' function was used. The seasonal patterns obtained from the decomposition of the series (two seasons per year) were considered. The analysis was carried out through time windows of 6 months considering the wet and dry season, using the 'slider :: slide_dbl' function. The functions used were from the statistical computer language R (Version 3.6.3), as well as the 'ggplot2' package used to visualize data and information. Finally, the percentage of windows showing positive rate of change was calculated, as shown below:

$$\%m = \frac{\sum_{i=1}^{N_i} x_i}{N_i} \quad (1)$$

where *x* is the positive slope for observing time window *i*, while *N* represents the number of time windows.

2.4 Relationship between drought based on DI and SPI

For evaluating the meteorological drought, the SPI index proposed by (McKee et al., 1993) was used , which classifies the severity of the drought in mild drought (0.00> SPI ≥ -0.99), moderate drought (-1.00> SPI ≥ -1.49), severe drought (-1.49> SPI ≥ -1.99) and extreme drought (-2.0> SPI). The precipitation from 2004 to 2016 (in mm/h) was obtained from the TRMM_3B43 data set

(https://daac.gsfc.nasa.gov/datasets/TRMM_3B43_7/summary).The SP index can be calculated at different time scales, such as 1, 3, 6, 12, 24, or 48 months(Jing et al., 2019). In this study, the SPI was used on a 1-month time scale adjusted to a gamma distribution, as expressed below:

$$SPI = Z_{ij} = \frac{y_{ij} - \bar{y}}{\bar{s}_i} \quad (2)$$

where the precipitation *y* is defined as a spatio-temporal variable composed of *j* monthly observations in each of the *i* locations, which characterizes a Z_{ij} score by subtracting the mean of *y* and dividing by the mean standard deviation.

The study area was zoned into three categories according to the rate of change of the bf: positive, neutral, and negative. First, the Pearson coefficient determined the correlation between the standardized DI at the sfsm level and the SPI considering annual time series. To determine if there are significant differences between correlations of SPI concerning DI, an ANOVA statistical analysis was applied.

2.5 Burned area and drought by ENSO intensity

To determine the burned areas in the Amazon basin, the areas were classified according to the humidity percentiles at the gws level, those with a humidity percentile less than 30% were considered as areas with drought, while the areas without drought were established as those with humidity greater than 30%. (Houborg et al. 2012). The total area burned for areas with drought and areas without drought was calculated according to the influence of the intensity of ENSO events. The years and intensities of the warm events (El Niño) for the period 2004-2016 were obtained based on the Oceanic Niño Index (ONI) (http://ggweather.com/enso/oni.htm). The threshold of anomalies + 0.5 ° is divided into events Weak (0.5 to 0.9), Moderate (1.0 to 1.4), Strong (1.5 to 1.9) and Very strong (≥2.0). During classification they considered the events must have occurred during at least 3 consecutive periods of 3 months. Based on the intensity of the ENSO, the years 2015-16 were classified as very strong ENSO years and the years 2009-10 as moderate ENSO years. Whereas the years 2004-05, 2006-07 and 2014-15 were considered years with weak ENSO

events and without ENSO events the years 2012-13 and 2013-14 (Taufik et al., 2017). During the study period, there were no strong ENSO events.

3 Results

3.1 Temporal variability of the hydrological drought

Throughout the study period, the average and minimum humidity percentiles show a clear tendency to decrease (Figure 2 a and b). Furthermore, compared to different soil levels, it is evident that the moisture percentiles increase with depth (Figure 2a). As evidenced in Figure 2b, drought events were more extreme in the subsoil (gws). For the three depth levels, the DI maintained the same seasonality pattern, showing a slight change in the trend at the subsoil level (Figure 2c).

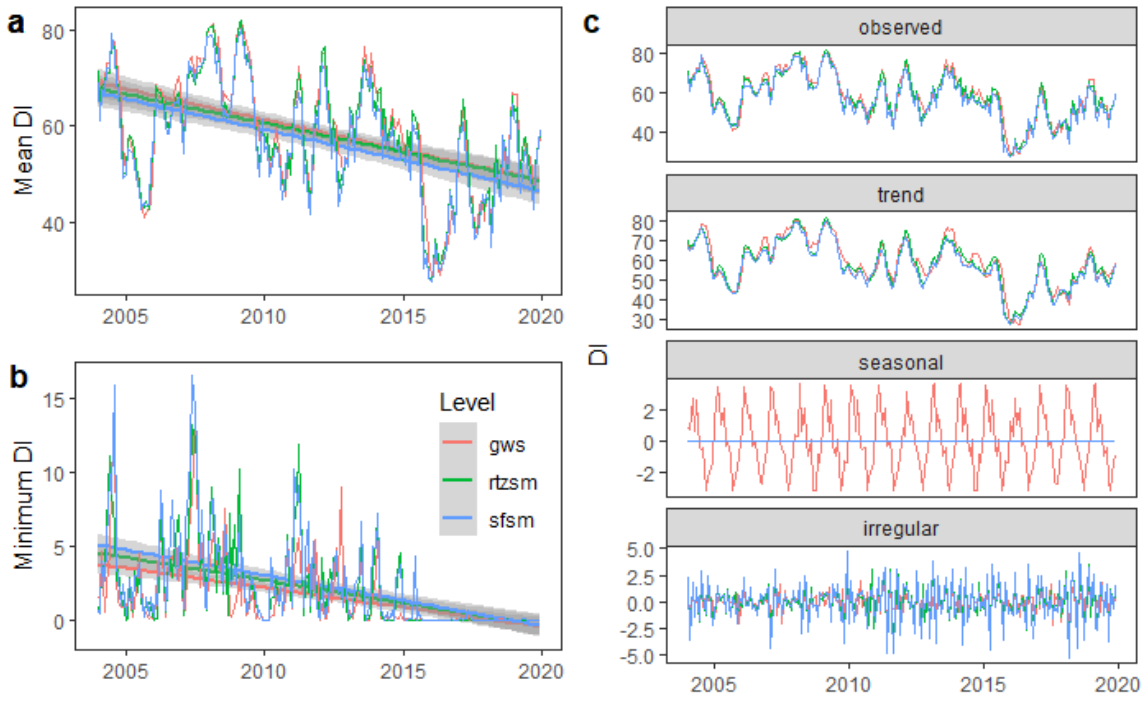

Figure 2. Temporal distribution of the Drought Indicator (DI) at the level of surface soil moisture (sfsm), root zone soil moisture (rtzsm) and groundwater (gws) for the years 2004-2019 in the Amazon basin. **a**, Annual average of the DI. **b**, Minimum percentiles of moisture of the DI. 95% confidence intervals (shaded area). **c**, DI decomposition to evaluate trends and seasonality patterns, as showed by the observed values, the trend to the evolution of

the series over time, the seasonal to fluctuations that are repeated every year, and the irregular to random fluctuations.

3.2 Relationship between DI and the extension of burned areas

The spatial distribution shows that the areas with lower humidity are concentrated in the Northeast of the Amazon basin at the subsoil level (gws and rtzsm) (Figure 3a). On the other hand, in the south of the basin there is a decrease in humidity at the surface level as showed in a black circle (Figure 3a, sfsm).

The Hydrological Drought Indicator DI showed a similar behavior at all levels of soil depth (Figure 3b), observing a decrease in humidity towards the East of the Amazon. On the other hand, in the south of the Amazon, the humidity conditions showed a positive rate of change at the surface level (sfsm), while at the subsoil level (gws) and root zone (rtzsm) the humidity decreased along throughout the entire period 2004-2016.

When evaluating the bf concerning the period 2004 to 2016, three kinds of zones were found (positive, neutral, and negative rates of change). The negative trend for the bf was mainly found in the south and southeast of the basin, while the positive trends for the increase in bf were found in the central part of the Amazon basin (Figure 3a, bf). On the other hand, for the bf evaluated by 6-month windows was found that up to 60% of the study period maintained positive rates of change in the south and southeast of the basin (Figure 3b, bf).

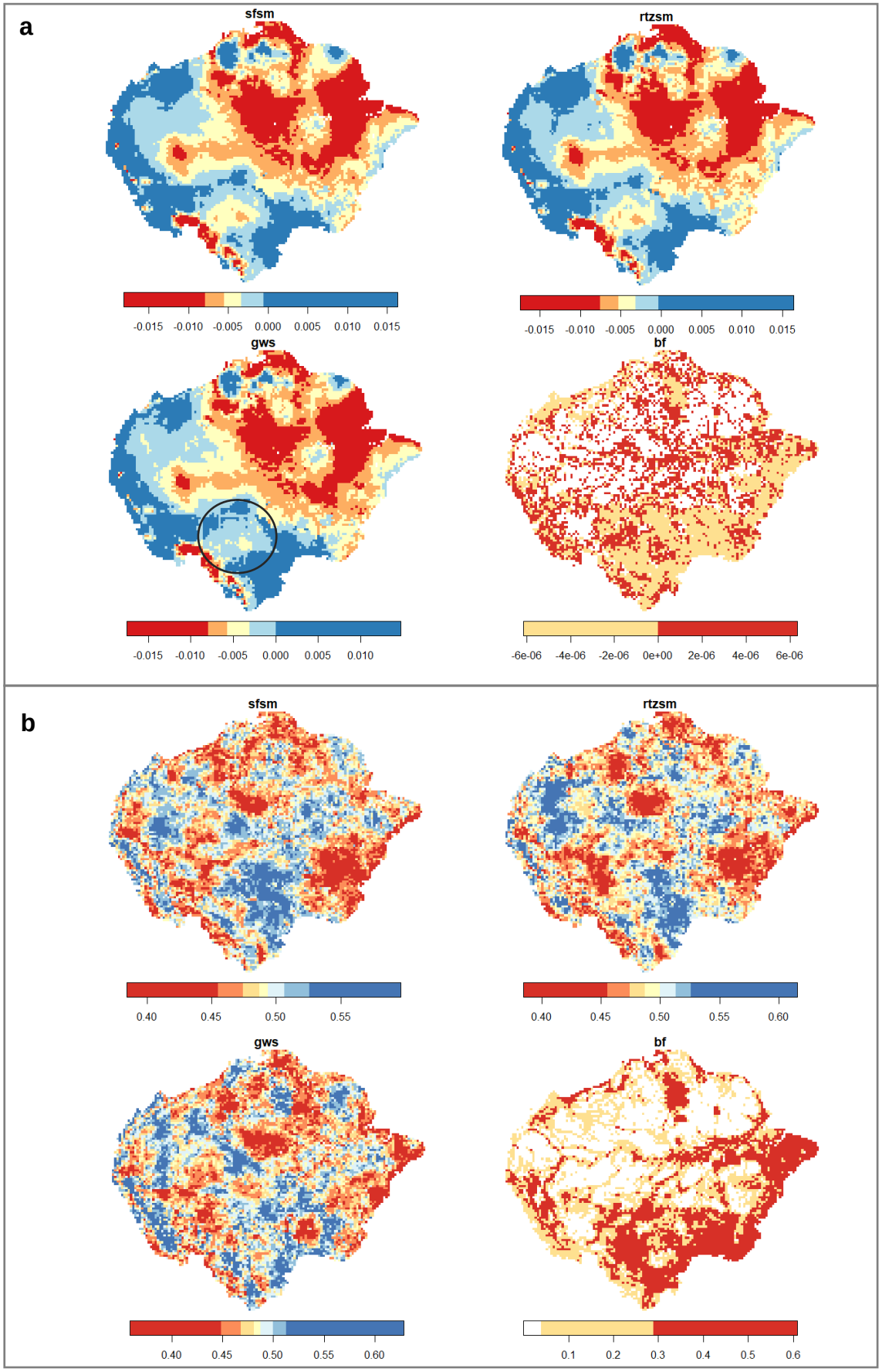

Figure 3. Spatial rate of change of the Hydrological Drought Indicator (DI) at the level of

surface soil moisture (sfsm), root zone soil moisture (rtzsm), and groundwater (gws), and the burned area fraction (bf) respect to the period from 2004 to 2016. a, rate of change average. b, percentage of time windows with positive rate of change (no fires occurred in areas with values <1%).

3.3 Relationship between hydrological and meteorological drought

Hydrological (measured by DI-sfsm) and meteorological (measured by SPI) droughts were correlated for the areas identified with positive, neutral and negative rates of change for the period studied. (Figure 4). The zone with a positive rate of change showed the highest correlation (R = 0.72, P <0.01). On the contrary, the correlation decreases for areas with neutral and negative rates of change. However, when applying the ANOVA to each zone, no significant differences were found for the SPI (F (1, 37) = 0.0001, P = 0.992,) and the DI-sfsm (F (1, 37) = 0.0241, P = 0.878).

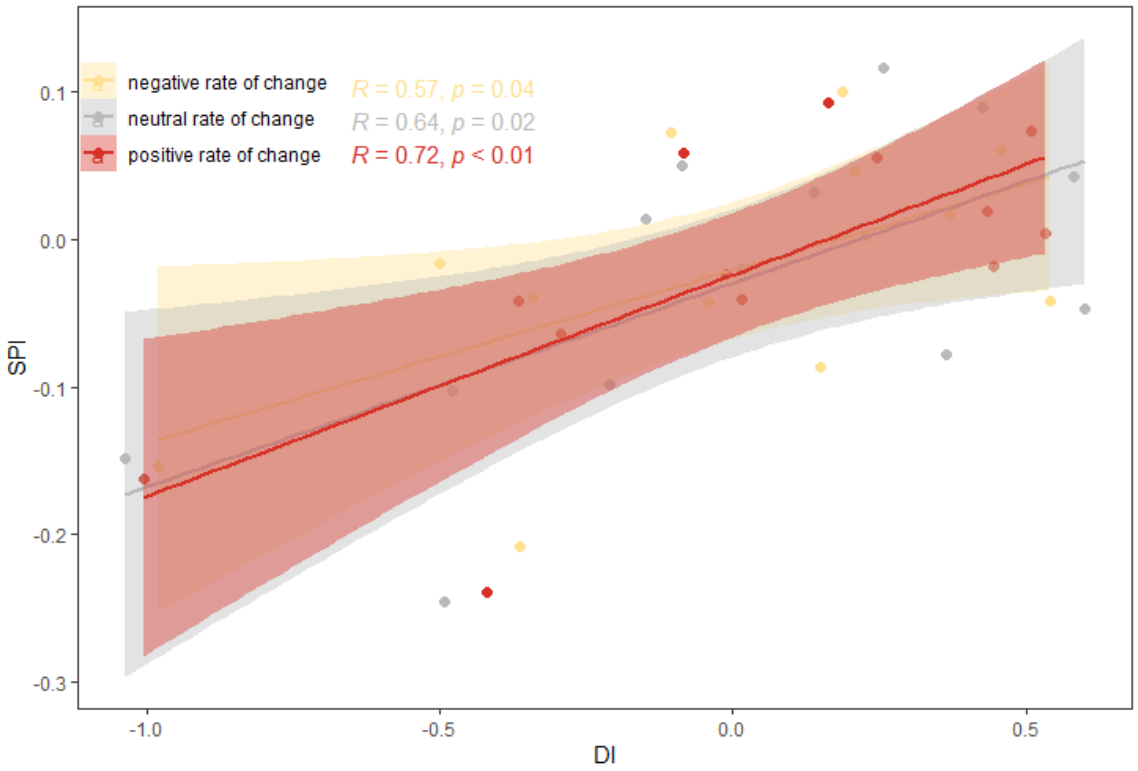

Figure 4. Correlation between DI and SPI according to the rate of change of the fraction of burned areas in the Amazon for the period 2004-2016. Where group with negative rate of change $(-\mathbf{6.13x10^{-6}}, -\mathbf{4.83x10^{-9}})$ indicates decrease in bf, neutral rate of change

$(-\mathbf{4.83x10^{-9}}, \mathbf{0})$ maintains bf and positive rate of change $(\mathbf{0}, \mathbf{6.33x10^{-6}})$ increment of bf. 95% confidence interval.

On average, the largest amount of burned area in the Amazon was found in areas where there was no hydrological drought (Figure 5). However, there is an amplification of the burned area in areas with drought during a strong ENSO event. It is also observed that the maximum burned area (1.5x10^5 ha) occurred during an ENSO event classified as "very strong" for areas that presented drought. Possibly due to during the ENSO phase, yhe anomalous warming over the equatorial Pacific alters the Walker Circulation from east to west, suppressing the precipitation in the Amazon basin (Ropelewski & Halpert, 1987). The prolonged absence of rain can generate extreme soil humidity conditions, generating a water stress in the plants that increases the mortality rates of the trees and greater susceptibility to flammability in the forests (Nepstad et al., 2008).

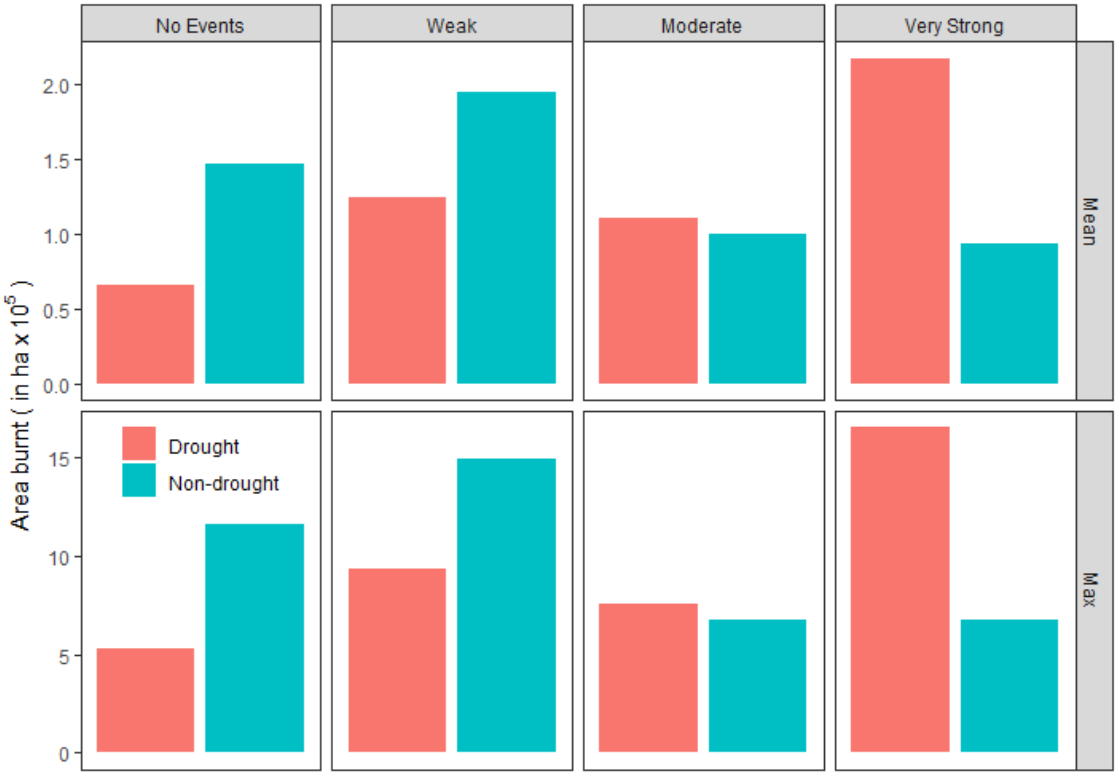

Figure 5. The average and maximum burned area for various intensities of ENSO events for areas with drought and no hydrological drought in the Amazon. The years 2012-13 and 2013-14 were classified without ENSO events; the years 2004-05, 2006-07 and 2014-15

were considered years with weak ENSO events; the years 2009-10 as moderate ENSO years; the years 2015-16 were considered as very strong ENSO years.

4 Discussion

The characterization of hydrological drought is limited in understanding the temporal dynamics of the humidity conditions in the subsoil, since these are not divided into components based on depth, but only based on data measured at the soil surface. Groundwater changes are known to be slower compared to precipitation changes (A. C. Thomas et al., 2014). This dynamic is corroborated in this study since the average DI tended to decrease the humidity conditions in the subsoil for the three depths, with the highest drought amplification being evidenced for the sfsm level. At the sfsm level it is known that soil moisture storage tends to be replaced more easily with precipitation (Taufik et al., 2017). As expected, the most extreme drought conditions were observed at a greater depth level (gws). It can then be suggested that the moisture deficits in the subsoil could be associated with future droughts because the groundwater zone is more vulnerable once the recharge is slower than the other zones.

The cases with a correlation between the SPI and the DI-sfsm are because DI-sfsm is based on surface-level humidity conditions and does not behave as a meteorological index. Zones with a positive change rate of the bf show the highest correlation (> 0.7); this could indicate that where both meteorological drought and hydrological drought occur, there is a trend towards the amplification of wildfires. Whereas the areas where the bf tends to decrease or fires did not occur, the meteorological drought is not proportional to the hydrological drought, showing correlation coefficients lower than 0.7. This wildfire increment is because when a meteorological drought event spreads, the groundwater recharge is reduced, increasing the soil's capillarity and decreasing the height of the water table. Consequently, biomass becomes fire-prone due to the drying of organic matter on the surface, which may increase the number of fires (Taufik et al., 2017).

Forest fires present complex dynamics, mainly when it is located in humid tropical forests (Fernandes et al., 2011). In the Amazon, forest fires coincide with hydrological drought events influenced by ENSO (Lopes et al., 2016; Taufik et al., 2017). However, forest fires also occur during years without drought, though their amplification in terms of burned area

and frequency occurs during years with drought (Taufik et al., 2017).This study shows that areas burned during hydrological drought events at the groundwater level could amplify with the increment of El Niño intensity. The period of 2015-2016 had a very strong El Niño intensity. Consequently, there was a 244% increment in the average annual burned area in areas with extreme drought compared to areas with non-drought conditions. In 2015, any warming anomaly observed in the last decade was overcome due to the combined effects of El Niño and the global warming trend, increasing the severity of the drought (Jiménez-Muñoz et al. 2016). Similarly, from 2004 to 2005, considered a period influenced by weak ENSO and anomalously warming of the Tropical North Atlantic, experienced significant drought (J. L. Chen et al., 2010). This same pattern was repeated for the years 2006 and 2009, where the minimum humidity coincided with the weak ENSO events. This information is critical and can help prepare the region for an increment in fires. The next step would be to develop a fire risk index for Amazonia using found data.

5 Conclusion

The hydrological drought tends to decrease the soil humidity conditions, being more extreme at the groundwater level. Highest frequency of hydrological drought occurred at the surface level, as a response of 1month long meteorological drought. Finally, the spread of fire within areas with extreme hydrological drought increases in proportion to the intensity of El Niño events.

References

Baker, I. T., Prihodko, L., Denning, A. S., Goulden, M., Miller, S., & Da Rocha, H. R. (2009). Seasonal drought stress in the amazon: Reconciling models and observations. *Journal of Geophysical Research: Biogeosciences*, *114*(1), 1–10. https://doi.org/10.1029/2007JG000644

Belal, A., & El-ramady, H. R. (2014). Drought risk assessment using remote sensing and GIS techniques, 35–53. https://doi.org/10.1007/s12517-012-0707-2

Benton, W. (Ed.). (1963). *Encyclopaedia Britannica*. University of Chicago Press.

Berenguer, E., Lennox, G. D., Ferreira, J., Malhi, Y., Aragão, L. E. O. C., Barreto, J. R., et al. (2021). Tracking the impacts of El Niño drought and fire in human-modified Amazonian forests. *Proceedings of the National Academy of Sciences of the United States of America*, *118*(30). https://doi.org/10.1073/pnas.2019377118

Changnon, J. (1987). Detecting Drought Conditions in Illinois.

Chen, J. L., Wilson, C. R., Tapley, B. D., Yang, Z. L., & Niu, G. Y. (2009). 2005 drought event in the Amazon River basin as measured by GRACE and estimated by climate models. *Journal of Geophysical Research: Solid Earth*, *114*(5), 1–9. https://doi.org/10.1029/2008JB006056

Chen, J. L., Wilson, C. R., & Tapley, B. D. (2010). The 2009 exceptional Amazon flood and interannual terrestrial water storage change observed by GRACE, *46*(April), 1–10. https://doi.org/10.1029/2010WR009383

Chen, Y., Chen, Y., Randerson, J. T., Morton, D. C., Defries, R. S., Collatz, G. J., et al. (2011). Forecasting Fire Season Severity in South America Using Sea Surface Temperature Anomalies, *787*. https://doi.org/10.1126/science.1209472

Chen, Y., Velicogna, I., Famiglietti, J. S., & Randerson, J. T. (2013). Satellite observations of terrestrial water storage provide early warning information about drought and fire season severity in the Amazon. *Journal of Geophysical Research: Biogeosciences*, *118*(2), 495–504. https://doi.org/10.1002/jgrg.20046

Dagum, E. B., & Bianconcini, S. (2010). *Seasonal Adjustment Methods and Real Time Trend-Cycle Estimation*. Retrieved from http://link.springer.com/10.1007/978-3-319-31822-6

Espinoza, J. C., Ronchail, J., Guyot, J. L., Junquas, C., Vauchel, P., Lavado, W., et al. (2011). Climate variability and extreme drought in the upper Solimões River (western Amazon Basin): Understanding the exceptional 2010 drought. *Geophysical Research Letters*, *38*(13), 1–6. https://doi.org/10.1029/2011GL047862

Fernandes, K., Baethgen, W., Bernardes, S., Defries, R., Dewitt, D. G., Goddard, L., et al. (2011). North Tropical Atlantic influence on western Amazon fire season variability, *38*, 1–5. https://doi.org/10.1029/2011GL047392

Gerdener, H., Engels, O., & Kusche, J. (2020). A framework for deriving drought indicators from the Gravity Recovery and Climate Experiment (GRACE), 227–248.

Houborg, R., Rodell, M., Li, B., Reichle, R., & Zaitchik, B. F. (2012). Drought indicators based on model-assimilated Gravity Recovery and Climate Experiment (GRACE) terrestrial water storage observations, *48*(June). https://doi.org/10.1029/2011WR011291

Jiménez-muñoz, J. C., Mattar, C., Barichivich, J., & Santamaría-, A. (2016). Record-breaking warming and extreme drought in the Amazon rainforest during the course of El Niño 2015 – 2016. *Nature Publishing Group*, (May), 1–7. https://doi.org/10.1038/srep33130

Jing, W., Yao, L., Zhao, X., Zhang, P., Liu, Y., Xia, X., et al. (2019). Understanding terrestrial water storage declining trends in the Yellow River Basin Key Points : by using GRACE satellites data and global models . weighted centroid analysis approach . by using the random forest algorithm ., (1). https://doi.org/10.1029/2019JD031432

Ladiray, D., & Quenneville, B. (2001). *Seasonal Adjustment with the X-11 Method*. *Bayesian Networks and Decision Graphs* (Vol. 13). Retrieved from https://books.google.ie/books?id=jzbY4NisxckC&printsec=frontcover&source=gbs_ge_summary_r&cad=0#v=onepage&q&f=false

Lopes, A. V, Chiang, J. C. H., Thompson, S. A., & Dracup, J. A. (2016). Trend and uncertainty in spatial-temporal patterns of hydrological droughts in the Amazon basin, 3307–3316. https://doi.org/10.1002/2016GL067738.Received

McKee, T., Doesken, N., & Kleist, J. (1993). The Relationship of Drought Frequency and Duration to Time Scales.

Nepstad, D. C., Stickler, C. M., Soares-Filho, B., & Merry, F. (2008). Interactions among Amazon land use, forests and climate: Prospects for a near-term forest tipping point. *Philosophical Transactions of the Royal Society B: Biological Sciences*, *363*(1498), 1737–1746. https://doi.org/10.1098/rstb.2007.0036

Nie, N., Zhang, W., Chen, H., & Guo, H. (2017). A Global Hydrological Drought Index Dataset Based on Gravity Recovery and Climate Experiment (GRACE) Data A Global Hydrological Drought Index Dataset Based on Gravity Recovery and Climate Experiment (GRACE) Data, (December). https://doi.org/10.1007/s11269-017-1869-1

Pappo, E., Wilson, C., & Flory, S. L. (2021). Hybrid coffee cultivars may enhance agroecosystem resilience to climate change. *AoB PLANTS*, *13*(2), 1–9. https://doi.org/10.1093/aobpla/plab010

Pontes-Lopes, A., Silva, C. V. J., Barlow, J., Rincón, L. M., Campanharo, W. A., Nunes, C. A., et al. (2021). Drought-driven wildfire impacts on structure and dynamics in a wet Central Amazonian forest. *Proceedings of the Royal Society B: Biological Sciences*, *288*(1951). https://doi.org/10.1098/rspb.2021.0094

Ropelewski, C. F., & Halpert, M. S. (1987). Global and regional scale precipitation patterns associated with the El-Nino Southern Oscillation. *Mon. Weather Rev*, *115(8)*, 1606–1626.

Tang, W., & Arellano, A. F. (2017). Investigating dominant characteristics of fires across the Amazon during 2005–2014 through satellite data synthesis of combustion signatures. *Journal of Geophysical Research*, *122*(2), 1224–1245. https://doi.org/10.1002/2016jd025216

Tapley, B. D., Watkins, M. M., Flechtner, F., Reigber, C., Bettadpur, S., Rodell, M., et al. (2019). Contributions of GRACE to understanding climate change. *Nature Climate Change*, (April). https://doi.org/10.1038/s41558-019-0456-2

Taufik, M., Torfs, P. J. J. F., Uijlenhoet, R., Jones, P. D., Murdiyarso, D., & Van Lanen, H. A. J. (2017). Amplification of wildfire area burnt by hydrological drought in the humid tropics. *Nature Climate Change*, *7*(6), 428–431. https://doi.org/10.1038/nclimate3280

Thomas, A. C., Reager, J. T., Famiglietti, J., & Rodell, M. (2014). A GRACE-based water storage deficit approach for hydrological drought characterization. *Geophysical Research Letters*, 1537–1545. https://doi.org/10.1002/2014GL059323.Received

Thomas, B. F., Famiglietti, J. S., Landerer, F. W., Wiese, D. N., Molotch, N. P., & Argus, D. F. (2017). Remote Sensing of Environment GRACE Groundwater Drought Index : Evaluation of California Central Valley groundwater drought. *Remote Sensing of Environment*, *198*, 384–392. https://doi.org/10.1016/j.rse.2017.06.026

Wang, L., Huang, G., & Chen, W. (2019). Towards a theoretical understanding of multiscalar drought indices based on the relationship between precipitation and standardized precipitation index. *Theoretical and Applied Climatology*, *136*(3–4), 1465–1473. https://doi.org/10.1007/s00704-018-2578-2

Yin, W., Li, T., Zheng, W., Hu, L., Han, S., & Tangdamrongsub, N. (2020). Improving regional groundwater storage estimates from GRACE and global hydrological models over Tasmania , Australia.

Yoon, J. H., & Zeng, N. (2010). An Atlantic influence on Amazon rainfall. *Climate Dynamics*, *34*(2), 249–264. https://doi.org/10.1007/s00382-009-0551-6

Zheng, W., Hsu, H., Zhong, M., & Yun, M. (2012). Efficient accuracy improvement of GRACE global gravitational field recovery using a new Inter-satellite Range Interpolation Method. *Journal of Geodynamics*, *53*, 1–7. https://doi.org/10.1016/j.jog.2011.07.003